PLOS ONE

RESEARCH ARTICLE

Effects of substrate stiffness and actin velocity on *in silico* fibronectin fibril morphometry and mechanics

Seth H. Weinberg[1]*, **Navpreet Saini**[2], **Christopher A. Lemmon**[2]*

1 Department of Biomedical Engineering, Ohio State University, Columbus, OH, United States of America,
2 Department of Biomedical Engineering, Virginia Commonwealth University, Richmond, VA, United States of America

* clemmon@vcu.edu (CAL); weinberg147@osu.edu (SHW)

Abstract

Assembly of the extracellular matrix protein fibronectin (FN) into insoluble, viscoelastic fibrils is a critical step during embryonic development and wound healing; misregulation of FN fibril assembly has been implicated in many diseases, including fibrotic diseases and cancer. We have previously developed a computational model of FN fibril assembly that recapitulates the morphometry and mechanics of cell-derived FN fibrils. Here we use this model to probe two important questions: how is FN fibril formation affected by the contractile phenotype of the cell, and how is FN fibril formation affected by the stiffness of the surrounding tissue? We show that FN fibril formation depends strongly on the contractile phenotype of the cell, but only weakly on *in vitro* substrate stiffness, which is an analog for *in vivo* tissue stiffness. These results are consistent with previous experimental data and provide a better insight into conditions that promote FN fibril assembly. We have also investigated two distinct phenotypes of FN fibrils that we have previously identified; we show that the ratio of the two phenotypes depends on both substrate stiffness and contractile phenotype, with intermediate contractility and high substrate stiffness creating an optimal condition for stably stretched fibrils. Finally, we have investigated how re-stretch of a fibril affects cellular response. We probed how the contractile phenotype of the re-stretching cell affects the mechanics of the fibril; results indicate that the number of myosin motors only weakly affects the cellular response, but increasing actin velocity results in a decrease in the apparent stiffness of the fibril and a decrease in the stably-applied force to the fibril. Taken together, these results give novel insights into the combinatorial effects of substrate stiffness and cell contractility on FN fibril assembly.

Introduction

Fibronectin plays a prominent role in embryonic development, wound healing, and disease

Fibronectin (FN) fibrils are the primordial extracellular matrix assembled by fibroblasts during wound healing and embryogenesis. In embryogenesis, FN fibrils are essential for some of the

earliest developmental steps: in Xenopus embryos, gastrulation fails in the absence of FN, and the embryos have significant cardiovascular defects [1]. In wound healing, the initial fibrin clot binds to factor XIII which in turn facilitates binding with FN [2]. FN fibrils serve both as a means of structurally stabilizing the clot [3] and as a network that facilitates cell migration into the wound to direct immune response and tissue building [4].

Cells stretch fibronectin to drive assembly into insoluble, viscoelastic fibrils

Fibronectin is a 250-kDa glycoprotein that is present in a soluble form at high concentration in the blood plasma [5]. Cells bind to soluble plasma fibronectin via transmembrane integrins. Mehanical force is applied to integrins via contraction of the actomyosin cytoskeleton, which transmits force via focal adhesions to integrins and then to FN [6]. Stretching FN exposes buried cryptic FN-FN binding sites, which leads to the incorporation of another soluble plasma FN [7]. This in turn leads to assembly of networks of viscoelastic, insoluble fibrils. Initial de novo assembly of FN fibrils requires soluble FN to be tethered; this tethering can be mediated by FN binding to Collagen I [8], FN binding to charged proteins via its highly charged III2-4 and III12-14 regions [9, 10] or by binding of the two FN integrin binding sites across neighboring, clustered integrins [11, 12].

Assembly of fibronectin fibrils is dependent on cell phenotype

Since FN fibrils require cell-derived traction forces to expose cryptic binding sites [6], and since different cell types generate differing magnitudes of contractile forces [13], it thus follows logically that the assembly of FN fibrils depends on the cell type. Previous studies have demonstrated that fibroblast and mesenchymal cells robustly assemble fibrils *in vitro*, while epithelial and endothelial cells exhibit negligible fibrillogenesis [13]. There is a bi-phasic response however; cells that generate the largest forces, such as smooth muscle cells and cardiomyocytes, also generate only minimal numbers of fibrils [13]. One way in which we can represent these cellular differences in contractile state is by varying actin velocity, specifically the unloaded velocity of an actin filament not tethered to a focal adhesion. Prior studies have demonstrated that this unloaded actin velocity varies over several orders of magnitude between differing cell types [14]. These studies show that cells with higher unloaded actin velocities correspond with myosin types that have been shown to exhibit higher contractility; a summary of unloaded actin velocities as a function of myosin type from this study is shown in Fig 1.

Assembled fibronectin fibrils alter the mechanoresponse of attached cells

Over the past two decades, there has been an increased understanding of the role that substrate stiffness plays in driving cellular mechanoresponses [15–17]. It is now well appreciated that cells on increasingly stiffer surfaces generate larger traction forces. FN fibrils play a key role in the sensing of substrate stiffness; when FN fibril assembly is inhibited, fibroblasts do not generate larger forces in response to increasing substrate stiffness [18]. Despite this key role in mechanosensing, there does not seem to be a correlation between substrate stiffness and the degree of FN assembly: previous studies from our group have demonstrated that cells will assemble FN fibrils across a range of substrate stiffness values, with only a slight dependence on substrate stiffness [18].

A computational model of fibronectin fibril formation captures in vitro fibril morphometry and mechanics

The mechanism of FN fibril assembly is still poorly understood. This is partially due to the fact that, as opposed to actin or tubulin which spontaneously assemble in cell-free environments,
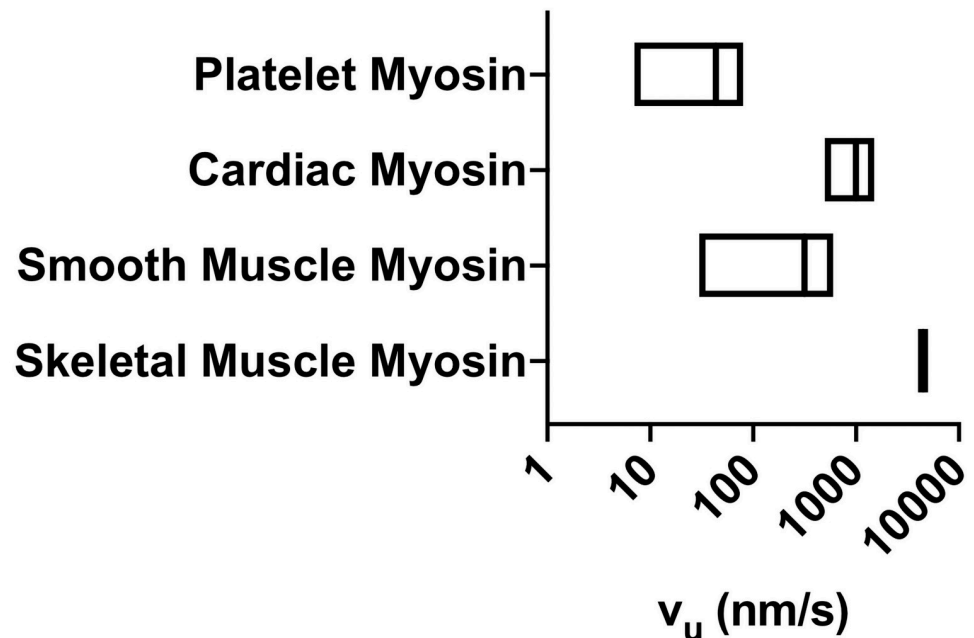
Fig 1. Unloaded actin velocities for given myosin types. Previously published studies [14] have demonstrated that actin velocity varies with myosin type and with the degree of myosin phosphorylation. Ranges represent the unphosphorylated (min) and phosphorylated (max) values of unloaded actin velocity, v_u.

https://doi.org/10.1371/journal.pone.0248256.g001

FN fibril assembly requires cell-generated forces, and is thus difficult to replicate in cell-free environments. While several groups have attempted to generate FN fibrils in cell-free environments by shearing soluble FN [19–21], these fibrils often exhibit different morphologies and mechanics from cell-derived FN fibrils. To probe the potential mechanism of FN fibril mechanics, we previously generated a computational model that constructs *in silico* FN fibrils from first principles [22]. This model was based on a previously developed motor-clutch model that simulated the interaction between the actomyosin contractile unit of the cell and the underlying substrate [23] and predicted cellular mechanical responses to various substrate stiffnesses. In our previous work, we integrated a fibronectin molecule between the cell and substrate, and then incorporated the mechanism of FN incorporation and fibril growth (shown in Fig 2, described further in Materials and Methods, and described fully in [22]). We then compared the morphology and mechanics of these simulated fibrils to cell-derived fibrils, and have shown that the simulated fibrils recapitulate many of the fibril properties, including fibril length, length-to-thickness ratio, and stretched-to-relaxed length ratio.

Previous studies suggest a potentially complex relationship between cell phenotype, substrate stiffness, and FN fibril formation. In the current work, we investigate these relationships by using our existing FN fibril assembly model to investigate the following questions: first, how does substrate stiffness affect FN fibril formation in our model? Our prior experimental work would suggest that the model should predict FN fibril assembly across a range of stiffness values. Second, how does cellular contractile phenotype, as characterized by the unloaded actin velocity, affect FN fibril assembly? Prior studies from our group and others have suggested that the contractile phenotype of the cell strongly affects FN fibril assembly, regardless of substrate stiffness. Finally, how does the contractile phenotype of a cell that is re-stretching a previously assembled fibril affect its mechanosensing response? In other words, if two cells of differing contractile phenotype migrate over an existing FN fibril and re-stretch it, do the cells
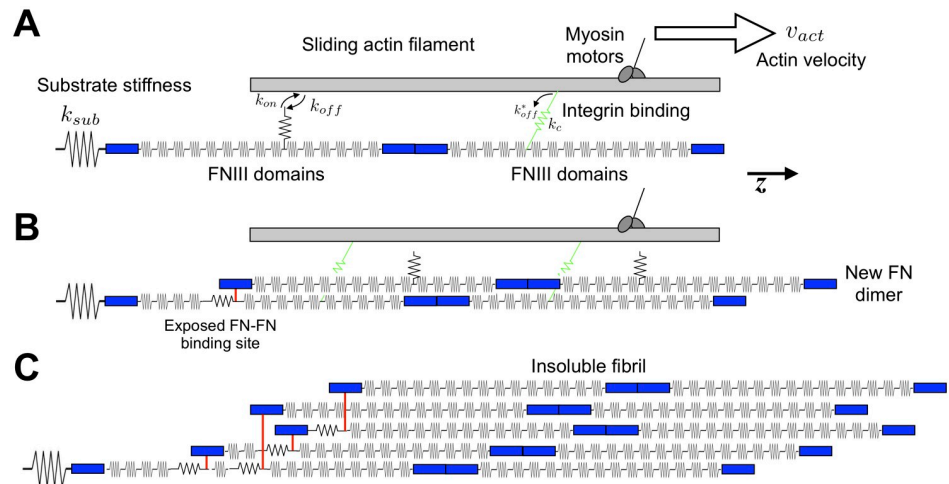
Fig 2. Diagram of computational model of FN fibril assembly. A schematic of the FN fibril assembly model used in the current study. A) Actomyosin machinery stochastically binds to FN at the III-10 domain, with a force-dependent k_{off}. B) This binding and pulling unfolds FN Type III domains, exposing cryptic FN-FN binding sites. C) This process continues until the system reaches equilibrium, such that the fibril, clutch and mysoin pulling force are balanced, and no new FN molecules are added.

"feel" a different fibril? By answering these questions, we can gather significant insight into the mechanism of FN fibril assembly in response to a range of mechanical environments and cellular phenotypes.

Materials and methods

Model formation

To simulate fibronectin fibril growth, we used a hybrid stochastic-deterministic model that we have previously developed [22]. A schematic of the model is shown in Fig 2. Briefly, we model an actin filament, pulled on by a myosin motor and coupled to a "clutch", which represents the collective focal adhesion/integrin complex. This clutch is attached to a single FN molecule, which in turn is coupled to the underlying tissue. The myosin motor pulling on the actin filament is modeled using the Hill force-velocity relationship, in which the resistive force is inversely proportional to the actin velocity:

$$v_{act} = v_u(1 - f_{sub}/f_{stall}), \qquad (1)$$

where f_{sub} is the force acting on the substrate, $f_{stall} = N_{myo}f_{myo}$ is a myosin stall force for which v_{act} approaches 0 and that is proportional to the number of myosin motors N_{myo} and individual myosin stall force f_{myo}, and v_u is the unloaded actin velocity.

The focal adhesion "clutch" is represented by Hookean springs in parallel, each of which has a force-dependent unbinding rate, which drives integrin/FN rupture proportional to force generation. The FN molecule is represented by 30 springs in series, which represent the elastic Type III domains in FN, which have previously been shown to unfold in response to force [24]. Finally, the tissue/substrate is modeled as a single Hookean spring, with substrate stiffness k_{sub}.

Simulations begin initially with a single (unbound) FN molecule, and the actin filament moving at its unloaded actin velocity v_u, a parameter of the simulation. The springs that comprise the clutch stochastically bind and unbind, attaching to the FN molecule, which in turn transmits force to the spring representing the substrate. The resultant motion generates a

reaction force. This reaction force alters both the speed of the actin filament and the binding/ unbinding kinetics of the focal adhesion clutch. The force also unfolds Type III domains in FN; once a domain has exceeded a length threshold (determined based on published steered molecular dynamics simulations of Type III domains [25]), it is deemed "open" and can bind a second FN molecule. This new molecule creates new binding sites for the focal adhesion/integrin clutch springs. The simulation proceeds until assembly is completed: that is, the fibril, clutch, and myosin pulling force are balanced such that no new addition of FN molecules occurs. In order to model the 3-dimensional aspect of an FN fibril, new FN molecules are added to the existing fibril using a hexagonal geometry. New FN molecules stochastically fill an empty site in the hexagonal pattern, and only FN molecules on the "outside" of the fibril are able to bind new FN molecules or integrin clutches (note that to the best of our knowledge, there is no experimental evidence as to the 3D packing of FN fibrils; we have used hexagonal packing of FN molecules in fibrils as a reasonable biological assumption). An in-depth discussion of the computational algorithm, including the handling of deterministic-stochastic coupling, can be found in the original publication of the model [22].

In this study, we have conducted new "re-stretching" simulations of *in silico* FN fibrils as follows: the result of the simulations above is a stretched FN fibril, with many Type III domains stretched open and binding to other FN molecules. To probe the mechanics of the FN fibrils, we "relax" these fibrils by resetting all FN Type III springs and the substrate spring to their resting lengths. This fibril is "re-stretched" by simulating the same myosin force, actin filament speed, and focal adhesion clutch binding as in the previous assembly simulations. Importantly, these parameters can differ from those used in the original simulation, allowing us to simulate a fibril assembled with one set of actomyosin parameters, but re-stretched with a different set of parameters. Note that in these re-stretching experiments, the addition of new FN molecules is inhibited.

Our prior studies have demonstrated two distinct FN fibril "phenotypes": one in which the simulation stabilizes at a constant FN fibril length with a constant applied force, which we have termed "Stably Stretched Fibrils (SSFs)"; and one in which the simulation never stabilizes, but stochastically fluctuates around a fibril length and applied force, which we have termed "Fluctuating Stretched Fibrils (FSFs)". Fig 3A shows a representative displacement vs. time plot for a fibril of each phenotype, Fig 3B shows a representative force vs. time plot for a representative fibril from each phenotype, and Fig 3C shows a representative force versus stretch plot for a representative fibril from each phenotype. An in-depth discussion of these two FN fibril phenotypes can be found in our prior work [26].

Model simulations

In the current work, we investigate two parameters: 1) the stiffness of the Hookean spring is changed to represent tissues of varying stiffness k_{sub}; 2) the unloaded actin velocity v_u, which is the speed at which myosin pulls the actin filament in the absence of any resistive force, is changed to represent different contractile phenotypes. A higher unloaded actin velocity represents a larger pulling force by myosin; previous experimental studies have demonstrated that unloaded actin velocity varies by several orders of magnitude from approximately 7 to 5000 nm/s, depending on cell type [14]. In a subset of experiments, the number of myosin motors N_{myo} was varied. For each combination of parameters, 100 simulations were run.

Results

Effects of substrate stiffness and actin velocity on FN fibril morphometry

We first investigated the effects of substrate stiffness and cellular phenotype by varying the stiffness of the spring that represents the underlying substrate (k_{sub}) and the unloaded actin
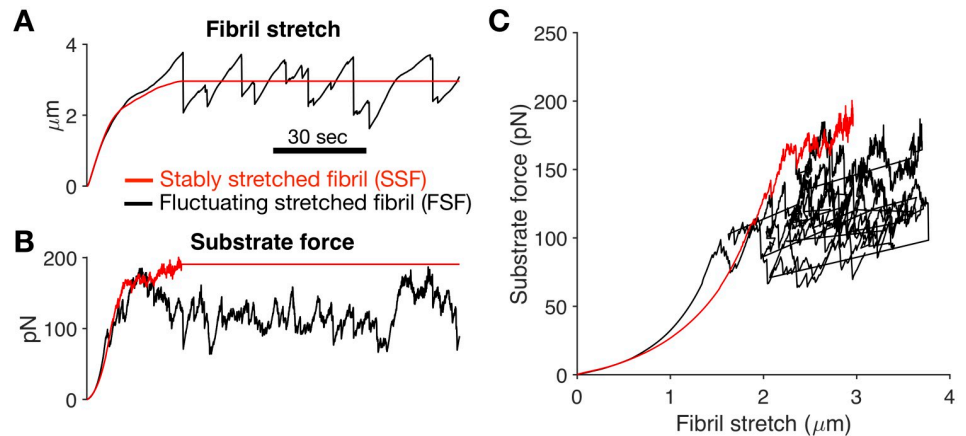
Fig 3. Stably stretched FN fibrils versus fluctuating stretched FN fibrils. In silico FN fibrils exhibit two distinct phenotypes. A) SSFs reach a stable stretch length, while FSF fluctuate around a central value; B) SSFs exhibit constant force transmission to the underlying substrate, while FSFs fluctuate; C) Force/displacement curves for a representative SSF (red) and FSF (black).

velocity of the pulling myosin motor (v_u), where a higher value represents a cell with a stronger contractile phenotype. Results from these simulations are shown in Fig 4. Mean values at the conclusion of the simulation are shown for each of the 100 simulations per condition for the following metrics: the total number of FN molecules that have been incorporated into the fibril (Fig 4A); the total force transmitted to the underlying substrate (Fig 4B); the length-to-thickness ratio of the fibril, which quantifies the geometry of the fibril (Fig 4C); the stretched length of the fibril, which represents the length while the fibril is still under cell tension (Fig 4D); the relaxed length, which represents the fibril length after release from cell tension (Fig 4E); the ratio of these two lengths, which indicates the extensibility of the fibril (Fig 4F); the fraction of clutches bound, which can be thought of as a corollary to the degree of integrin attachment to the fibril (Fig 4G); the length of the region from first attachment to last attachment to the fibril, which can be thought of as a corollary to focal adhesion length (Fig 4H); and finally, the time in hours until the simulated fibril reaches a steady state length (Fig 4I). All reported values show a strong correlation with the unloaded actin velocity v_u, but little to no dependence on substrate stiffness. The one exception is the FN fibril assembly time, which shows negligible dependence on either substrate stiffness or actin velocity.

To further analyze this response, we averaged each output in Fig 4 for a given actin velocity, regardless of substrate stiffness (Fig 5). Data indicate small variations at all actin velocities except for v_u = 10,000 nm/s, demonstrating that substrate stiffness does not dramatically affect FN mophometry, except at extremely high actin velocities. The data also reveal several interesting trends: as actin velocity increases, FN fibrils generated are smaller, as indicated by both the total number of FN molecules (Fig 5A) and the total stretched and relaxed fibril length (Fig 5D and 5E). As actin velocity increases, the forces transmitted through the fibril decreases (Fig 5B), the percentage of bound integrin clutches decreases (Fig 5G), and the average focal adhesion length decreases (Fig 5H). These data suggest that as actin velocity increases, there is an increased frequency of rupture at the integrin/FN bond, and that this results in reduced fibril assembly and transmitted force to the substrate. This indicates that our model is able to capture a counter-intuitive experimental finding that cells with an extremely pronounced contractile phenotype assemble shorter, thicker FN fibrils [27]. This potentially explains why cells that
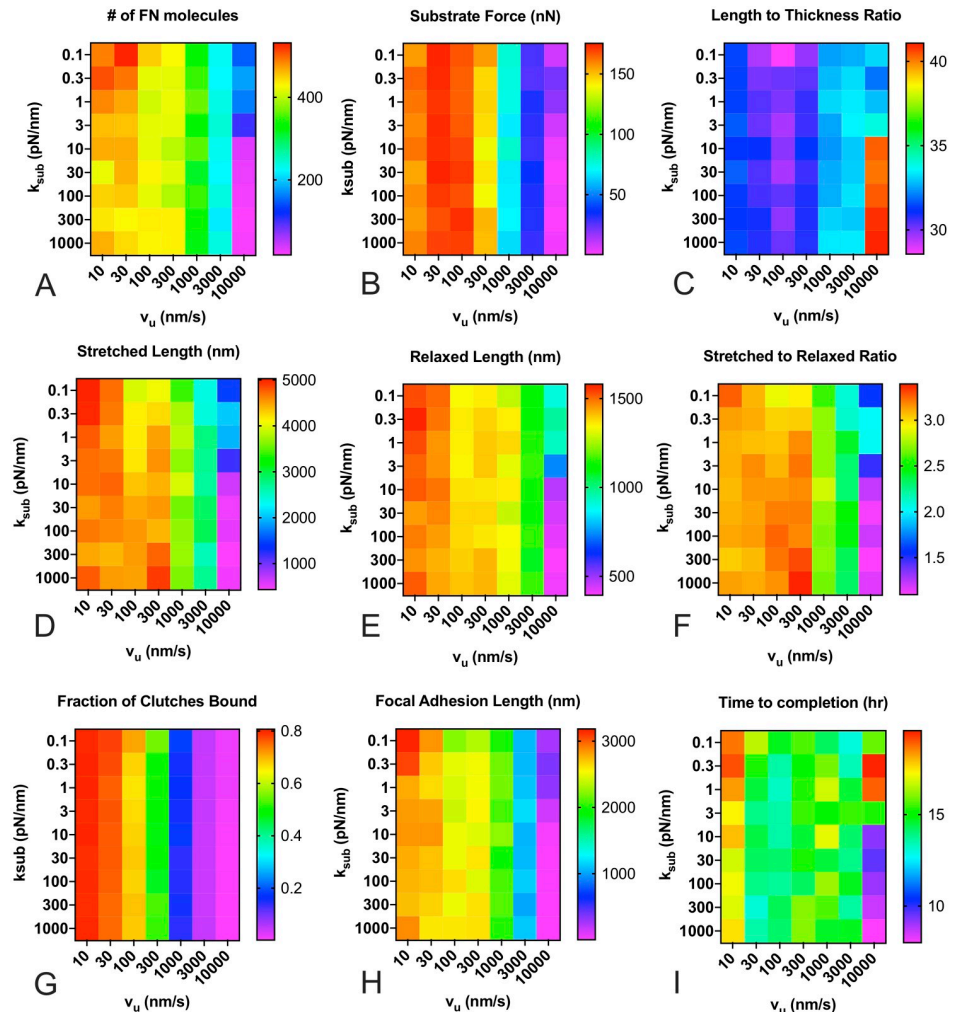
Fig 4. FN fibril morphometry as a function of substrate stiffness and actin velocity. Actin velocity has a pronounced effect, while substrate stiffness only shows a significant effect at extremely high actin velocities for (A) number of FN molecules in the FN fibril; (B) force transmitted via fibril to the substrate; (C) length to thickness ratio of the stretched fibril; (D) stretched length of the fibril; (E) relaxed length of the fibril; (F) stretched to relaxed ratio; (G) fraction of transmembrane clutches bound to the fibril; (H) length of focal adhesion attached to the fibril; and (I) time for FN fibril to reach steady-state. Each condition is the mean of 100 simulations.

https://doi.org/10.1371/journal.pone.0248256.g004

generate large contractile forces, such as smooth muscle cells and cardiomyocytes, exhibit negligible FN fibrilogenesis.

Effects of substrate stiffness and actin velocity on FN fibril restretching mechanics

We next examined whether changing substrate stiffness or actin velocity had effects on the mechanics of FN fibrils. To investigate this, we again simulated assembly of 100 fibrils per condition as above. We then "relaxed" the fibrils by releasing tension on the FN fibril springs, resetting each spring to zero displacement. These fibrils were re-stretched at the same actin velocity that was used to assemble the fibril. Re-stretching simulations were run for up to 5 minutes, or until the fibril "stalled" at a specific stretch length and force (i.e., the actin velocity falling less than 1% of the unloaded velocity). The resulting displacement and force generation
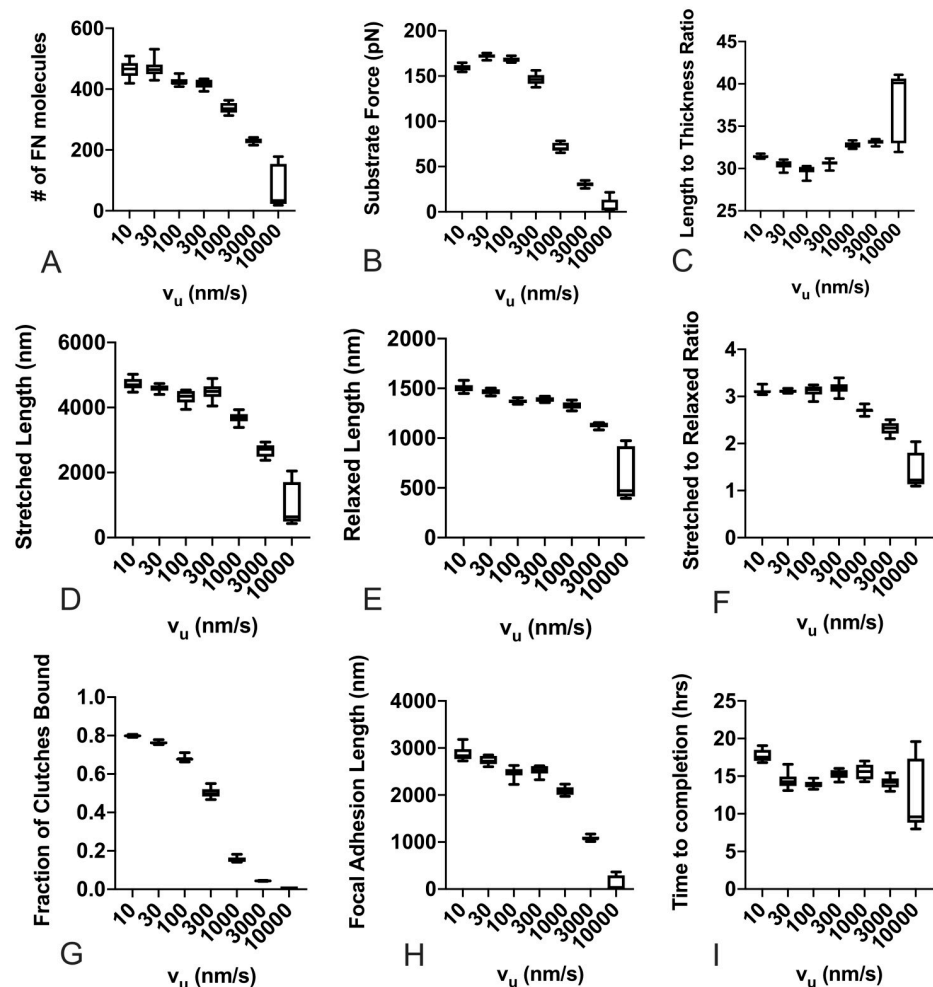
Fig 5. Effects of actin velocity on FN fibril morphometry and mechanics across all substrate stiffness values.
Effects of unloaded actin velocity, regardless of substrate stiffness on (A) number of FN molecules in the FN fibril; (B) force transmitted via fibril to the substrate; (C) length to thickness ratio of the stretched fibril; (D) stretched length of the fibril; (E) relaxed length of the fibril; (F) stretched to relaxed ratio; (G) fraction of transmembrane clutches bound to the fibril; (H) length of focal adhesion attached to the fibril; and (I) time for FN fibril to reach steady-state. Each box and whisker point shows the mean (line), the 25th—75th percentile range (box), and the min and max (whiskers) for 900 simulations (100 simulations for each of 9 stiffness values).

https://doi.org/10.1371/journal.pone.0248256.g005

were calculated to generate a force-displacement curve for each fibril. Data from a representative re-stretch simulation is shown in Fig 6.

Stress in the fibril was calculated by dividing force by the maximum fibril cross sectional area, and strain was calculated as fibril stretch divided by the unstretched fibril length. The slope of the stress-strain curve gives a measurement of the fibril elastic modulus or "stiffness". For analysis, we compared the stress-strain curve slope at the initiation of stretch. Fig 7 shows the mean value of A) the initial slope of the force-displacement curve, B) the mean stress at the end of re-stretching, C) the mean strain at the end of re-stretch, and D) the mean fibril displacement at the end of stretching. Results indicate that substrate stiffness again has little effect, while actin velocity has a pronounced effect on FN fibril mechanics.

Given this predominance of actin velocity on FN fibril mechanics, we again analyzed the effects on FN fibril mechanics as solely a function of actin velocity, regardless of substrate
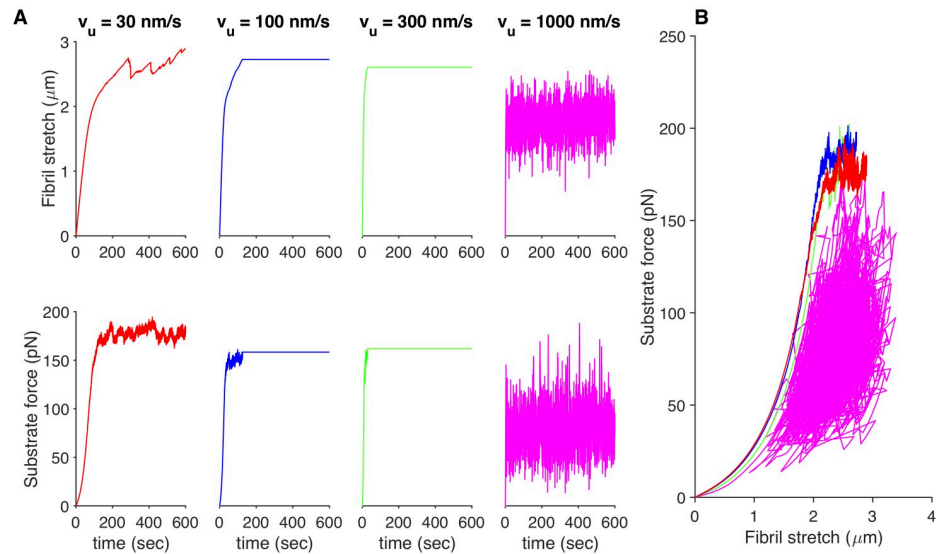
Fig 6. Determining the mechanical properties of FN fibrils by re-stretch simulation. *In silico* fibrils were generated as described above. After FN fibril assembly termination, fibrils were reset to their relaxed length and restretched using the same unloaded actin velocity value that was used during assembly. (A) representative stretch and force plots for 4 different unloaded actin velocities. (B) Force-displacement curves for the 4 fibrils shown in (A).

stiffness (Fig 8). Results indicate that the initial slope of the force-displacement curve, which indicates the initial apparent stiffness as the fibril is first stretched, decreases as actin velocity increases. This suggests that cells with a more contractile phenotype assemble less rigid fibrils, although this effect is small. Fibril stress and strain both show a maximum at intermediate values of actin velocity, suggesting that there is an unloaded actin velocity value in the 100-300 nm/s range in which fibrils exhibit a maximum stress and strain. Fibril displacement at the end of stretch only weakly depends on actin velocity, but decreases at large actin velocities.

Effects of substrate stiffness and actin velocity on FN fibril phenotype

Taken together, there are three conclusions that can be drawn from the results presented so far: first, substrate stiffness has minimal effects on FN fibril morphometry and FN fibril mechanical properties; second, increasing actin velocity yields FN fibrils that are smaller and softer; and third, an intermediate unloaded actin velocity exists at which stress and strain in the fibril are maximal. We next sought to determine the effects of substrate stiffness and actin velocity on FN fibril phenotype. As discussed above, we have previously identified two distinct FN fibril phenotypes: SSFs, which remain statically stretched, and FSFs, which fluctuate around a value of force and stretch length. Fig 9A shows the fraction of FN fibrils that exhibit the SSF phenotype. Results show a dependence on both substrate stiffness and actin velocity: at either low or high actin velocities, the phenotype is independent of substrate stiffness and is predominantly FSFs, but at intermediate actin velocities, the phenotype strongly depends on substrate stiffness: the percentage of SSFs increases with increasing substrate stiffness.

Effects of cell restretching properties on fibril mechanics

Cells can assemble FN fibrils, and then migrate away from them, leaving them to be re-stretched by other migrating cells. We next investigated whether the apparent properties of an assembled fibril changed depending on the contractile state of the cell. For these experiments,
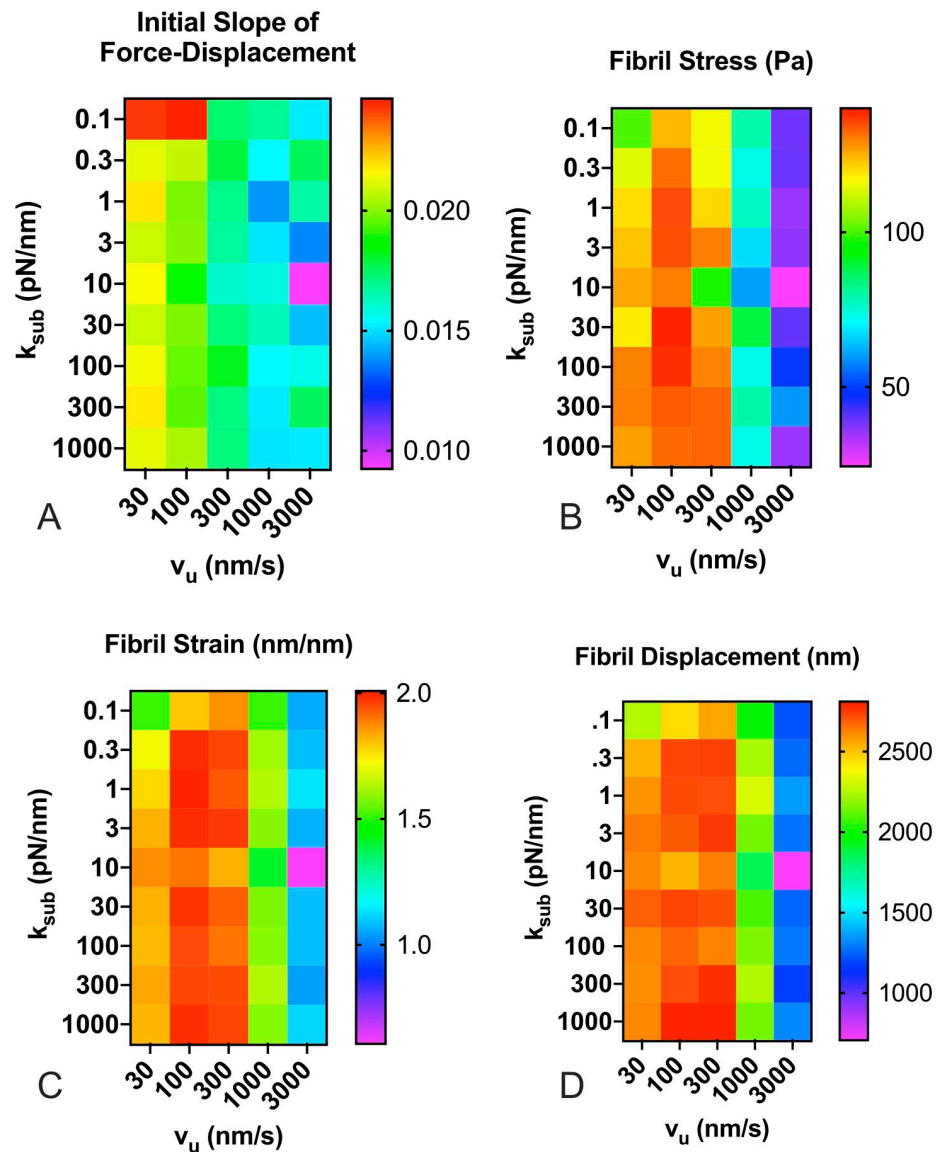
Fig 7. FN fibril mechanics as a function of substrate stiffness and actin velocity. Fibrils were computationally "relaxed", and then restretched at the same actin velocity used to assemble the fibril to quantify fibril mechanics. Actin velocity had a pronounced effect, while substrate stiffness had only a moderate effect on (A) the initial slope of the force-displacement curve, (B) the fibril stress at full stretch, (C) fibril strain at full stretch, and (D) fibril displacement. Each condition is the mean of 100 simulations.

https://doi.org/10.1371/journal.pone.0248256.g007

we used a population of 100 fibrils that were generated under the same conditions: an unloaded actin velocity of 300 nm/s, a substrate stiffness of 1000 pN/nm, and 100 myosin motors. These fibrils were released of any tension, and then re-stretched as explained above. The re-stretching of fibrils was performed over a range of values for the number of myosin motors and the unloaded actin velocity. Results, shown in Fig 10, indicate that the apparent mechanics of the re-stretched fibril is only minimally affected by the number of myosin motors. However, the actin velocity has pronounced effects. To probe the effects of actin velocity, data was re-analyzed as a function of actin velocity only, regardless of the number of myosin motors (Fig 11). Several interesting trends can be observed. First, there is an optimal actin
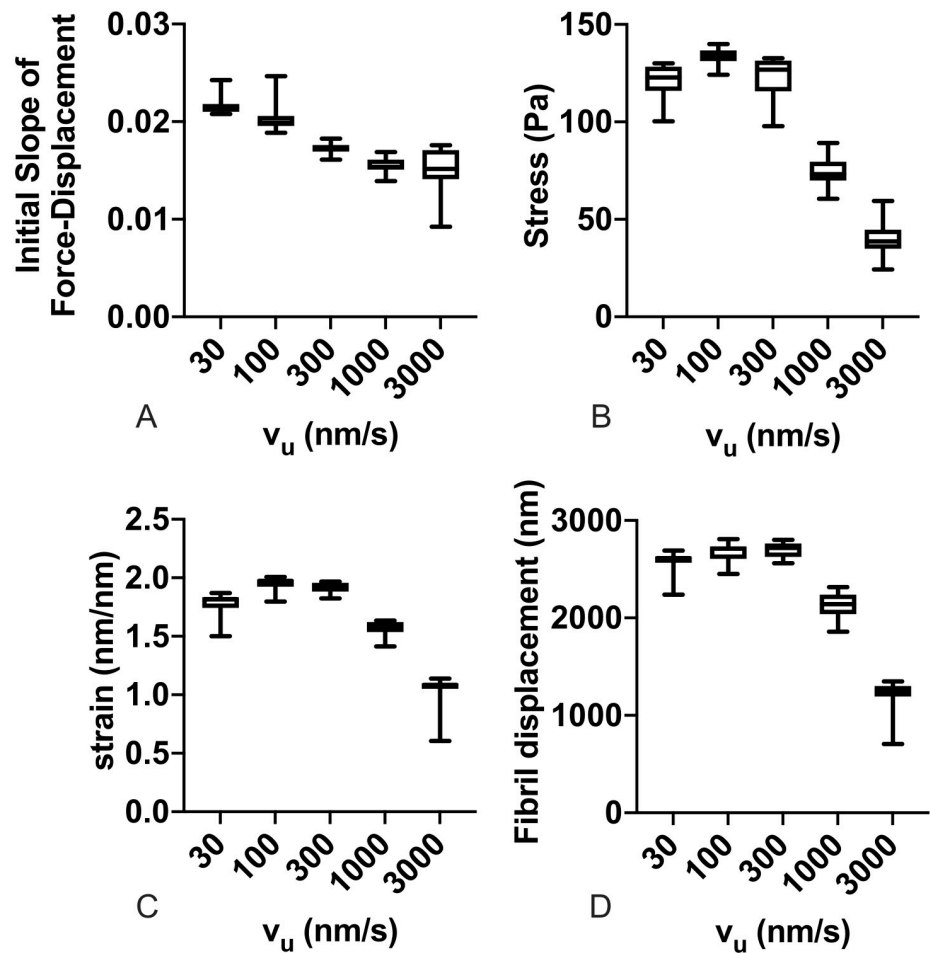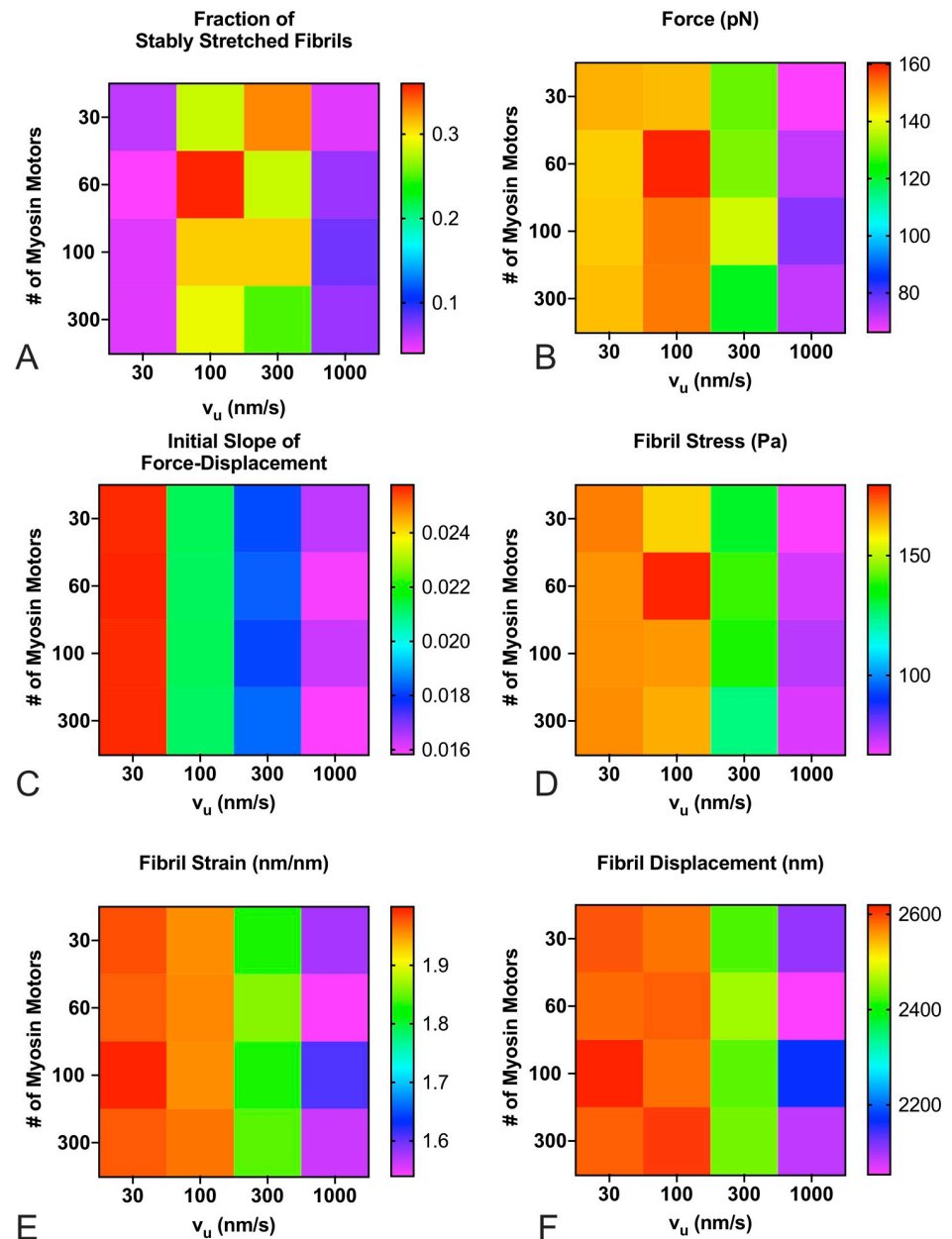
Fig 8. FN fibril mechanics as a function of actin velocity. Effects of unloaded actin velocity, regardless of substrate stiffness for (A) the initial slope of the force-displacement curve, (B) the fibril stress at full stretch, (C) fibril strain at full stretch, and (D) fibril displacement. Each box and whisker point shows the mean (line), the 25th—75th percentile range (box), and the min and max (whiskers) for 900 simulations (100 simulations for each of 9 stiffness values).
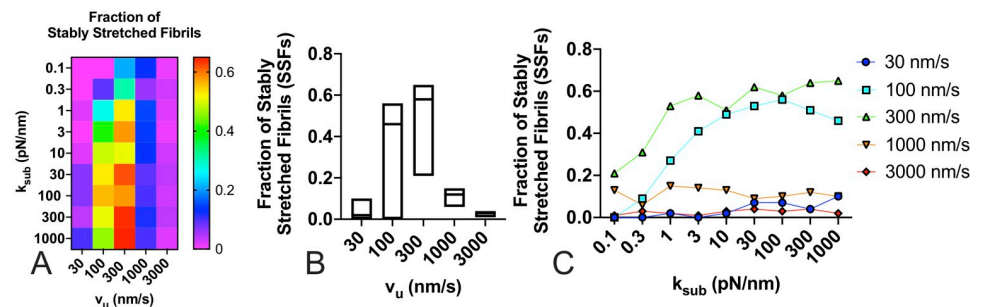
Fig 9. Fraction of stably stretched FN fibrils as a function of substrate stiffness and actin velocity. The fraction of fibrils that exhibited the SSF phenotype was determined for (A) both substrate stiffness and actin velocity; (B) actin velocity alone), and (C) as a function of substrate stiffness for each unloaded actin velocity.
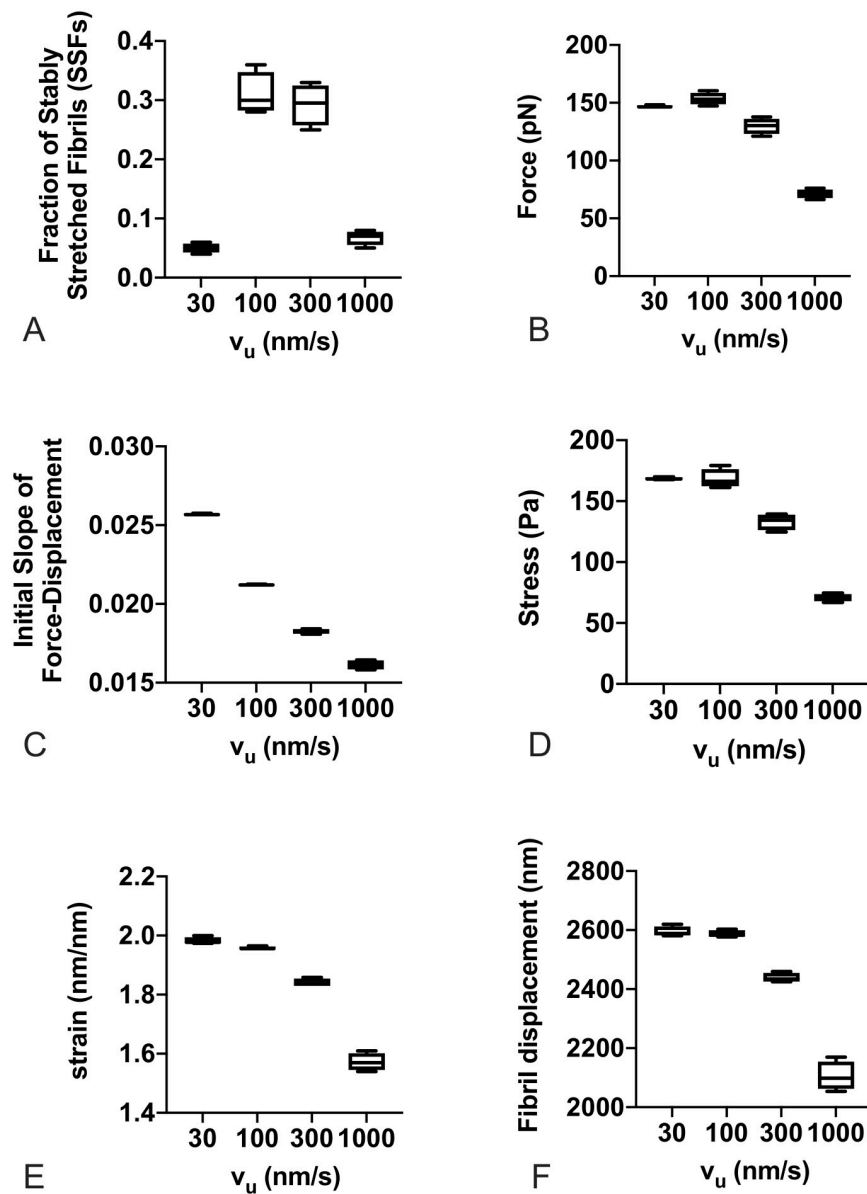
Fig 10. FN fibril morphometry and mechanics as a function of actin velocity and number of myosin motors. The number of myosin motors has minimal effects, while the unloaded actin velocity has significant effects on (A) the fraction of SSFs; (B) force transmitted via fibril to the substrate; (C) the initial slope of the force-displacement curve; (D) fibril stress; (E) fibril strain; and (F) fibril displacement. Each condition is the mean of 100 simulations.

velocity at which the percentage of stably stretched fibrils is maximal (Fig 11A). This suggests that the fibril phenotype depends on both the fibril itself as well as the phenotype of the cell that is stretching it. Second, increasing actin velocity, which corresponds with a cell with an increased contractile phenotype, results in fibrils that have reduced steady state force (Fig 11B), reduced apparent stiffness (Fig 11C), reduced stress (Fig 11D), reduced strain (Fig 11E), and reduced displacement (Fig 11F). This somewhat counter-intuitive result suggests that a

Fig 11. FN fibril morphometry and mechanics as a function of actin velocity. Actin velocity has a pronounced effect on (A) the fraction of SSFs; (B) force transmitted via fibril to the substrate; (C) the initial slope of the force-displacement curve; (D) fibril stress; (E) fibril strain; and (F) fibril displacement. Each condition is the mean of 100 simulations.

https://doi.org/10.1371/journal.pone.0248256.g011

cell with a stronger contractile phenotype will stretch a fibril less and exert less steady state force on the fibril compared to a cell with a lower contractile phenotype.

Discussion

In the current work, we have used a previously-developed computational model of FN fibril assembly to investigate the effects of both substrate stiffness and cellular contractile phenotype on fibril growth and mechanics. We have found that our model, based on first principles of force-driven FN stretching and assembly, predicts that the morphology and mechanics of FN

fibrils depend strongly on the contractile phenotype and only weakly on substrate stiffness. *In silico* experiments demonstrate that as contractility increases, assembled fibrils are smaller, with a shorter length, fewer FN molecules, and a lower fraction of attached integrin clutches. Our results also demonstrate that increasing contractility decreases the stiffness of the fibril. Both stress and strain within the fibril exhibit a maximal value at intermediate contractility, with both low and high contractile states resulting in lower stresses and strains.

We have also examined how substrate stiffness and contractility alter the proportion of two previously identified FN fibril phenotypes: SSFs and FSFs. Our data demonstrates that the proportion of fibrils in each phenotype depends on both substrate stiffness and contractility. At high or low contractility, FSFs are the predominant phenotype. At intermediate contractility, the percentage of SSFs increases with increasing substrate stiffness.

Finally, we have examined the effects of cellular contractile phenotype on the re-stretch of previously assembled FN fibrils. Results indicate that the unloaded actin velocity of the re-stretching cell affects the fibrils: a more strongly contracting phenotype results in fibrils that are less stretched and have a lower steady-state force magnitude.

One significant impact of the current work is that it provides a mechanistic explanation of two counter-intuitive experimental observations. First, previous studies have shown a bi-phasic response of FN fibril assembly to contractile force magnitude: knocking out traction forces with either myosin inhibitors or actin disrupters results in no FN fibril assembly [6]; but, increasing contractile force also leads to a reduction in FN fibril assembly [27]. Similarly, both cells that generate weak contractile forces, such as epithelial cells, and cells that generate large contractile forces, such as smooth muscle cells, exhibit minimal assembly of FN fibrils [13, 28]. Consistent with this, our model shows no FN fibril assembly at a non-contractile state, that is, $v_u = 0$, and shows that as cell contractility increases in the model, cells assemble fibrils that are smaller and shorter. Results demonstrate that as actin velocity increases, the fraction of cluthces bound to the fibril decrease, suggesting that decreased FN assembly at higher actin velocities is driven by more frequent rupture events at the integrin/FN interface.

Given that cellular traction forces increase with substrate stiffness [29, 30], and cellular traction forces drive FN fibril assembly [13], another experimental finding that is perhaps counter-intuitive is that FN fibrillogenesis does not depend strongly on substrate stiffness [31]. Our data again support this experimental finding, demonstrating that substrate stiffness only weakly affects FN morphology and mechanics. Our model suggests that the viscoelasticity of the fibril acts to "buffer" the substrate stiffness; as we have previously described [22], the FN assembly model results in an intermediate mechanics regime in which the presence of the fibril makes a soft surface "appear" stiffer, and a stiff surface "appear" softer. As such, assembly of FN fibrils may serve as a mechanism for mesenchymal cells to adjust and tailor their response to the surrounding tissue mechanics.

While the current work recapitulates several key experimental findings, it fails to accurately predict certain aspects of the FN/force/stiffness relationship. For example, while we have previously demonstrated that FN assembly is not dramatically affected by substrate stiffness, we and others have shown that traction forces still increase in response to increasing substrate stiffness when FN fibril assembly occurs [29, 31]. However, our model predicts that force transmitted via the fibril does not depend on substrate stiffness at all. One possible explanation is that we are predicting the mechanics and morphology of a single FN fibril. A cell attached to a surface will have tens to hundreds of attachments, and thus tens to hundreds of FN fibrils. Our model does not account for or predict the effects of multiple fibrils; thus, it is possible that in the described experimental work, each FN fibril transmits a similar magnitude of traction force, but that increased substrate stiffness results in more fibrils, and thus a larger total force applied to the substrate.

Of particular interest is the role that the two identified FN fibril phenotypes play in mechanotransduction, and how these phenotypes are affected by contractility and substrate stiffness. One could imagine that the cellular response to an FSF, in which the strain and force transmitted to the attached cell are fluctuating randomly, and an SSF, in which the fibril is tonically stretched and a constant force is transmitted, could be dramatically different. Our findings that: SSFs are only assembled in substantial number at an intermediate contractility; restretched fibrils exhibit SSF behavior at an intermediate contractile phenotype; and the fraction of SSFs increases with increasing stiffness, suggest that FN fibrils may be optimally tuned to provide mechanical cues at a given contractile state. Cells that cannot maintain this state, either by generating less force or by generating more force, do not assemble SSFs, and thus may lose a key mechanism to sense substrate stiffness. Investigation of FN fibril mechanics and phenotype, both experimentally and computationally, represents an active area of future work for our group.

Conclusion

Using a computational model of fibronectin fibril formation, we demonstrate that actin velocity, and in turn contractile phenotype, have a much more profound effect on fibril formation than substrate stiffness. Our work also demonstrates that both substrate stiffness and actin velocity/ contractility affect the ratio of two FN fibril phenotypes. At both low and high contractility, cells predominantly assemble fluctuating stretched fibrils (FSFs), while at intermediate contractility, cells assemble more stably stretched fibrils (SSFs), with the percentage of SSFs increasing with substrate stiffness. Together, these results give new insights into how substrate stiffness and cell contractility govern the assembly of FN fibrils.

Understanding the complex relationship between substrate stiffness, contractility, and FN assembly is key to understanding states for which FN assembly is desirable, such as wound healing and tissue engineering applications, as well as understanding conditions for which FN assembly is not desirable, such as the desmoplastic extracellular matrix of a growing tumor, the fibrotic response to implanted material within the body, and scar tissue in fibrotic disease.

Author Contributions

Conceptualization: Seth H. Weinberg, Christopher A. Lemmon.

Data curation: Navpreet Saini, Christopher A. Lemmon.

Formal analysis: Seth H. Weinberg, Navpreet Saini, Christopher A. Lemmon.

Funding acquisition: Seth H. Weinberg, Christopher A. Lemmon.

Investigation: Navpreet Saini.

Methodology: Christopher A. Lemmon.

Project administration: Seth H. Weinberg, Christopher A. Lemmon.

Software: Seth H. Weinberg.

Supervision: Christopher A. Lemmon.

Writing – original draft: Seth H. Weinberg, Christopher A. Lemmon.

Writing – review & editing: Seth H. Weinberg, Christopher A. Lemmon.

References

1. Marsden M, DeSimone DW. Regulation of cell polarity, radial intercalation and epiboly in Xenopus: novel roles for integrin and fibronectin. Development (Cambridge, England). 2001; 128(18):3635–47. https://doi.org/10.1242/dev.128.18.3635 PMID: 11566866

2. Clark RAF, An JQ, Greiling D, Khan A, Schwarzbauer JE. Fibroblast Migration on Fibronectin Requires Three Distinct Functional Domains. Journal of Investigative Dermatology. 2003; 121(4):695–705. https://doi.org/10.1046/j.1523-1747.2003.12484.x PMID: 14632184

3. Grinnel F. Fibroblast cell-substratum interactions: Role of cold insoluble globulin (plasma fibronectin). Experientia. 1980; 36(5):505–507. https://doi.org/10.1007/BF01965766 PMID: 6991273

4. Clark RA, Lanigan JM, DellaPelle P, Manseau E, Dvorak HF, Colvin RB. Fibronectin and fibrin provide a provisional matrix for epidermal cell migration during wound reepithelialization. The Journal of investigative dermatology. 1982; 79(5):264–9. https://doi.org/10.1111/1523-1747.ep12500075 PMID: 6752288

5. Mao Y, Schwarzbauer JE. Fibronectin fibrillogenesis, a cell-mediated matrix assembly process. Matrix Biology. 2005; 24(6):389–399. https://doi.org/10.1016/j.matbio.2005.06.008 PMID: 16061370

6. Zhong C, Chrzanowska-Wodnicka M, Brown J, Shaub A, Belkin AM, Burridge K. Rho-mediated Contractility Exposes a Cryptic Site in Fibronectin and Induces Fibronectin Matrix Assembly. The Journal of Cell Biology. 1998; 141(2):539–551. https://doi.org/10.1083/jcb.141.2.539 PMID: 9548730

7. Erickson HP. Stretching fibronectin. Journal of muscle research and cell motility. 2002; 23(5-6):575–80. https://doi.org/10.1023/A:1023427026818 PMID: 12785106

8. Dzamba BJ, Wu H, Jaenisch R, Peters DM. Fibronectin binding site in type I collagen regulates fibronectin fibril formation. J Cell Biol. 1993; 121(5):1165–72. https://doi.org/10.1083/jcb.121.5.1165 PMID: 8501121

9. Nelea V, Kaartinen MT. Periodic beaded-filament assembly of fibronectin on negatively charged surface. J Struct Biol. 2010; 170(1):50–9. https://doi.org/10.1016/j.jsb.2010.01.009 PMID: 20109553

10. Pernodet N, Rafailovich M, Sokolov J, Xu D, Yang NL, McLeod K. Fibronectin fibrillogenesis on sulfonated polystyrene surfaces. J Biomed Mater Res A. 2003; 64(4):684–92. https://doi.org/10.1002/jbm.a.10394 PMID: 12601780

11. Singh P, Carraher C, Schwarzbauer JE. Assembly of fibronectin extracellular matrix. Annu Rev Cell Dev Biol. 2010; 26:397–419. https://doi.org/10.1146/annurev-cellbio-100109-104020 PMID: 20690820

12. Wu C, Hughes PE, Ginsberg MH, McDonald JA. Identification of a new biological function for the integrin alpha v beta 3: initiation of fibronectin matrix assembly. Cell Adhes Commun. 1996; 4(3):149–58. https://doi.org/10.3109/15419069609014219 PMID: 8969861

13. Lemmon CA, Sniadecki NJ, Ruiz S, Tan JL, Romer LH, Chen CS. Shear force at the cell-matrix interface: enhanced analysis for microfabricated post array detectors. Mechanics & chemistry of biosystems: MCB. 2005; 2(1):1–16.

14. Cuda G, Pate E, Cooke R, Sellers J. In vitro actin filament sliding velocities produced by mixtures of different types of myosin. Biophysical Journal. 1997; 72(4):1767–1779. https://doi.org/10.1016/S0006-3495(97)78823-4 PMID: 9083681

15. Engler AJ, Sen S, Sweeney HL, Discher DE. Matrix Elasticity Directs Stem Cell Lineage Specification. Cell. 2006; 126:677–689. https://doi.org/10.1016/j.cell.2006.06.044 PMID: 16923388

16. Fu J, Wang YK, Yang MT, Desai RA, Yu X, Liu Z, et al. Mechanical regulation of cell function with geometrically modulated elastomeric substrates. Nature Methods. 2011; 7(9):733–736. https://doi.org/10.1038/nmeth.1487

17. Chen CS. Mechanotransduction—a field pulling together? Journal of Cell Science. 2008; 121 (20):3285–3292. https://doi.org/10.1242/jcs.023507 PMID: 18843115

18. Scott LE, Mair DB, Narang JD, Feleke K, Lemmon CA. Fibronectin fibrillogenesis facilitates mechano-dependent cell spreading, force generation, and nuclear size in human embryonic fibroblasts. Integrative biology: quantitative biosciences from nano to macro. 2015; 7(11):1454–65. https://doi.org/10.1039/c5ib00217f PMID: 26412391

19. Little WC, Smith ML, Ebneter U, Vogel V. Assay to mechanically tune and optically probe fibrillar fibronectin conformations from fully relaxed to breakage. Matrix Biology. 2008; 27(5):451–461. https://doi.org/10.1016/j.matbio.2008.02.003 PMID: 18417335

20. Feinberg AW, Parker K. Surface-initiated assembly of protein nanofabrics. Nano letters. 2010; 10 (6):2184–91. https://doi.org/10.1021/nl100998p PMID: 20486679

21. Salmerón-Sánchez M, Rico P, Moratal D, Lee TT, Schwarzbauer JE, García AJ. Role of material-driven fibronectin fibrillogenesis in cell differentiation. Biomaterials. 2011; 32(8):2099–2105. https://doi.org/10.1016/j.biomaterials.2010.11.057 PMID: 21185593

22. Weinberg SH, Mair DB, Lemmon CA. Mechanotransduction dynamics at the cell-matrix interface. Biophysical journal. 2017; 112(9):1962–1974. https://doi.org/10.1016/j.bpj.2017.02.027 PMID: 28494966

23. Chan CE, Odde DJ. Traction Dynamics of Filopodia on Compliant Substrates. Science. 2008; 322:1687–1691. https://doi.org/10.1126/science.1163595 PMID: 19074349

24. Abu-Lail NI, Ohashi T, Clark RL, Erickson HP, Zauscher S. Understanding the elasticity of fibronectin fibrils: unfolding strengths of FN-III and GFP domains measured by single molecule force spectroscopy. Matrix biology: journal of the International Society for Matrix Biology. 2006; 25(3):175–84. https://doi.org/10.1016/j.matbio.2005.10.007 PMID: 16343877

25. Gao M, Craig D, Vogel V, Schulten K. Identifying Unfolding Intermediates of FN-III10 by Steered Molecular Dynamics. Journal of Molecular Biology. 2002; 323(5):939–950. https://doi.org/10.1016/S0022-2836(02)01001-X PMID: 12417205

26. Lemmon CA, Weinberg SH. Multiple Cryptic Binding Sites are Necessary for Robust Fibronectin Assembly: An In Silico Study. Scientific reports. 2017; 7(1):18061. https://doi.org/10.1038/s41598-017-18328-4 PMID: 29273802

27. Lemmon CA, Chen CS, Romer LH. Cell Traction Forces Direct Fibronectin Matrix Assembly. Biophysical Journal. 2009; 96(2). https://doi.org/10.1016/j.bpj.2008.10.009 PMID: 19167317

28. Griggs LA, Hassan NT, Malik RS, Griffin BP, Martinez BA, Elmore LW, et al. Fibronectin fibrils regulate TGF-β1-induced epithelial-mesenchymal transition. Matrix Biology. 2017; 60:157–175. https://doi.org/10.1016/j.matbio.2017.01.001 PMID: 28109697

29. Saez A, Buguin A, Silberzan P, Ladoux B. Is the Mechanical Activity of Epithelial Cells Controlled by Deformations or Forces? Biophysical Journal. 2005; 89(6):L52–L54. https://doi.org/10.1529/biophysj.105.071217 PMID: 16214867

30. Califano JP, Reinhart-King CA. Substrate Stiffness and Cell Area Predict Cellular Traction Stresses in Single Cells and Cells in Contact. Cellular and molecular bioengineering. 2010; 3(1):68–75. https://doi.org/10.1007/s12195-010-0102-6 PMID: 21116436

31. Scott LE, Mair DB, Narang JD, Feleke K, Lemmon CA. Fibronectin fibrillogenesis facilitates mechano-dependent cell spreading, force generation, and nuclear size in human embryonic fibroblasts. Integrative biology: quantitative biosciences from nano to macro. 2015; 7:1454–65. https://doi.org/10.1039/c5ib00217f PMID: 26412391